Antikaon absorption in nuclear medium: role of hadron self-energies and implications for kaonic atoms

Jaroslava Óbertová

Faculty of Nuclear Sciences and Physical Engineering,
Czech Technical University in Prague

in collaboration with

Àngels Ramos
University of Barcelona

Eliahu Friedman
Hebrew University, Jerusalem

Jiří Mareš
NPI, Řež

SPICE workshop, 13 - 17 May 2024, Trento, Italy

This project has received funding from the European Union's Horizon 2020 research and innovation programme under grant agreement No 824093

K^-N interaction

- K^-N interaction near threshold described by chiral coupled-channel interaction models

  A. Cieply, J. Smejkal, NPA 881 (2012) 115 - Prague (P)

  Y. Ikeda, T. Hyodo, W. Weise, NPA 881 (2012) 98 - Kyoto-Munich (KM)

  A. Feijoo, V. Magas, A. Ramos, PRC 99 (2019) 035211 - Barcelona (BCN)

  Z. H. Guo, J. A. Oller, PRC 87 (2013) 035202 - Murcia (M1 and M2)

  M. Mai, U.-G. Meißner, NPA 900 (2013) 51 - Bonn (B2 and B4)

- Info about K^-N interaction below threshold provided by kaonic atoms

  65 data points (energy shifts, widths, yields=upper level widths) from CERN, Argonne, RAL, BNL

- Chirally motivated models fail to describe kaonic atom data

  E. Friedman, A. Gal, NPA 959 (2017) 66

Multinucleon processes

- Chiral models include only $K^- N \to \pi Y$ ($Y = \Lambda, \Sigma$) decay channel
- K^- interactions with two and more nucleons should be included, (e.g., $K^- + N + N \to Y + N$) $\leftarrow$ analysis of kaonic atom data

  E. Friedman, A. Gal, NPA 959 (2017) 66

$$V^{\rm phen}_{K^-{\rm multiN}} = -4\pi B(\frac{\rho}{\rho_0})^\alpha \rho$$

B is a complex amplitude, ρ is nuclear density distribution, ρ_0 is saturation density and α is positive

- equally good description of data with $\chi^2/{\rm d.p} \leq 2$

Single- vs. multi-nucleon processes

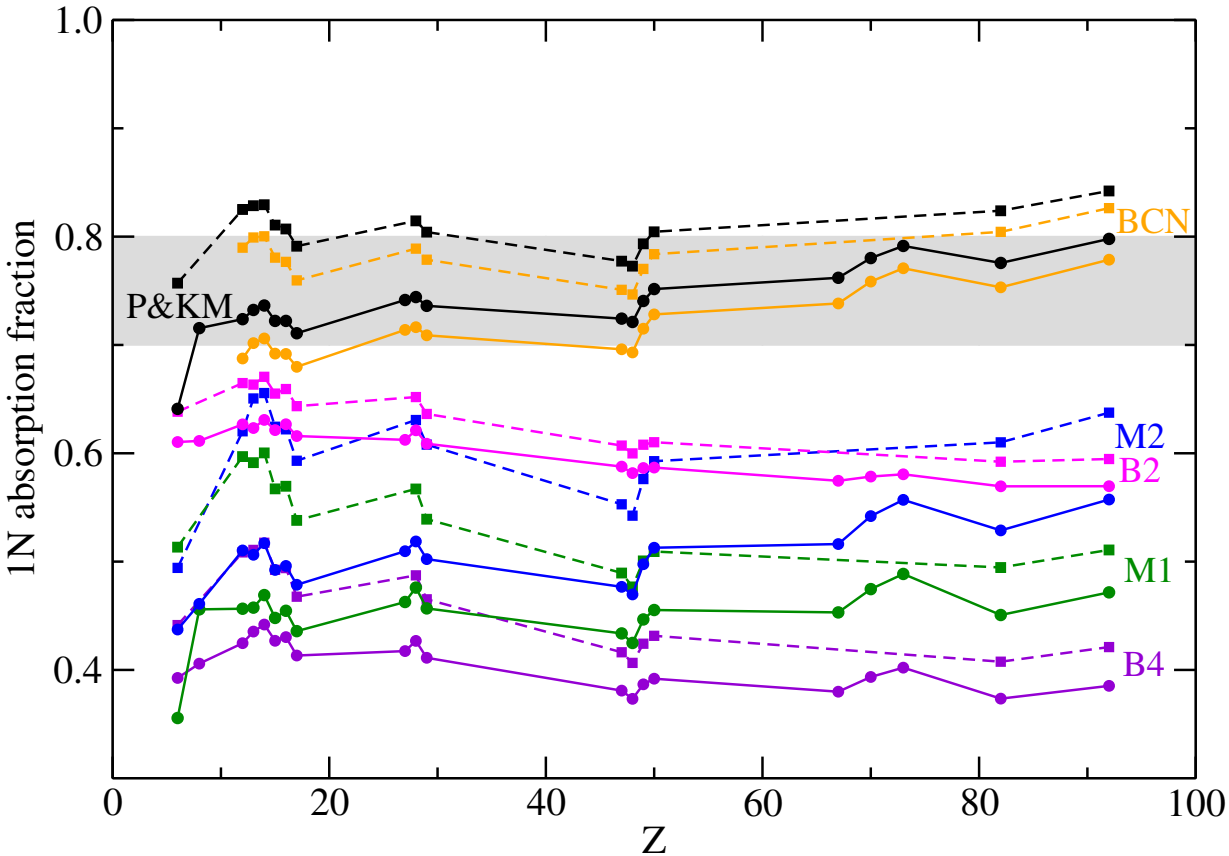

- Fraction of *single-nucleon* absorption 0.75 ± 0.05 (average value) used as an additional constraint.

$\rightarrow$ Only P, KM and BCN models found acceptable in kaonic atom analysis

E. Friedman, A. Gal, NPA 959 (2017) 66

K. Piscicchia, talk at THEIA-STRONG2020 Web-Seminar,20 December 2020

Outcome of the measurement

Investigated using: K^- "n" $^3He \rightarrow \Lambda\pi^- {}^3He$

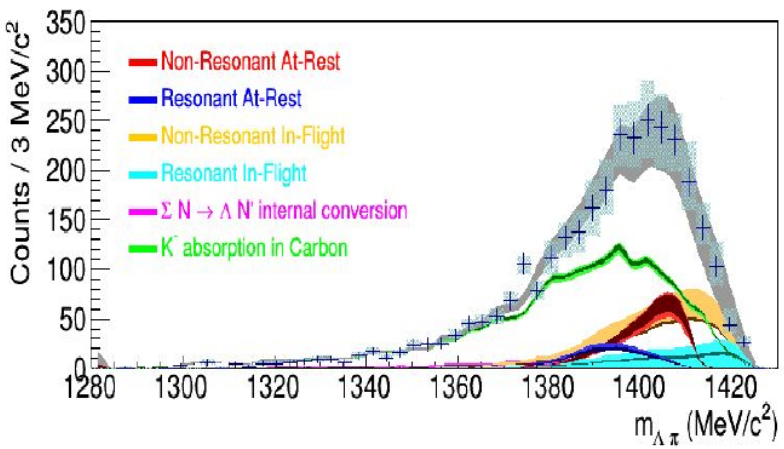

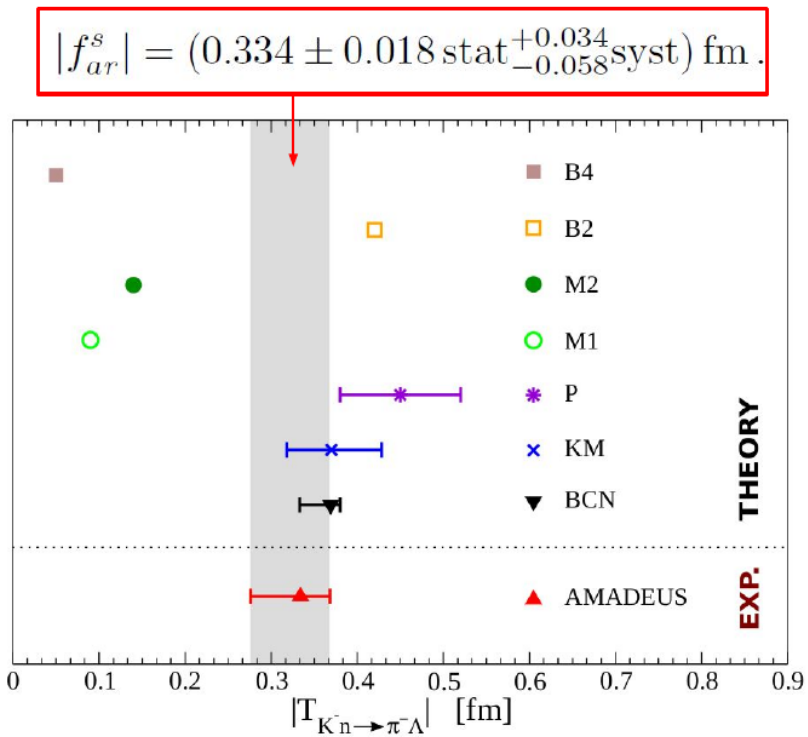

[K. Piscicchia, S. Wycech, L. Fabbietti et al. Phys.Lett. B782 (2018) 339-345]
[K. Piscicchia, S. Wycech, C. Curceanu, Nucl. Phys. A 954 (2016) 75-93]

25

Multinucleon processes

- K^- multi-nucleon absorption in the surface region of atomic nuclei represents about 20%

  NC 53 (1968) 313 (Berkeley), *NPB 35 (1971) 332 (BNL)*, *NC 39A (1977) 538 (CERN)*

- K^- multi-nucleon absorption in atoms described by phenomenological optical potential

  E. Friedman, A. Gal, NPA 959 (2017) 66

- Model for K^-NN absorption in nuclear matter using free-space chiral amplitudes

  T. Sekihara et al., PRC 86 (2012) 065205

- New experimental data on K^-NN absorption (AMADEUS@DAΦNE)

  K. Piscicchia et al., PLB 782 (2018) 339

  R. Del Grande et al., EPJ C79 (2019) 190

- Solid microscopic model for K^-NN absorption needed!

Microscopic model for K^-NN absorption in nuclear matter

Microscopic model for K^- two-nucleon absorption in symmetric nuclear matter *J. Hrtánková, À. Ramos, PRC 101 (2020) 035204*

- based on a meson-exchange approach
  H. Nagahiro et al., PLB 709 (2012) 87
- P and BCN chiral K^-N amplitudes employed
- Pauli correlations in the medium for K^-N amplitudes considered
- real part of the K^-NN optical potential evaluated as well
- K^-N optical potential derived within the same approach

$K^- N$ absorption in nuclear matter

$$K^- N \to \pi Y \quad (Y = \Lambda, \Sigma)$$

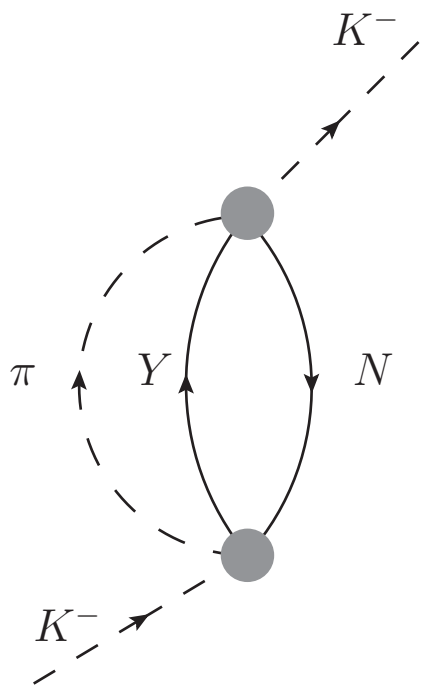

Fig.1: Feynman diagram for K^- absorption on a single nucleon in nuclear matter. The shaded circles denote the $K^- N$ t-matrices derived from a chiral model.

K^-NN absorption in nuclear matter

$$K^- + N + N \to Y + N \quad (Y = \Lambda, \Sigma)$$

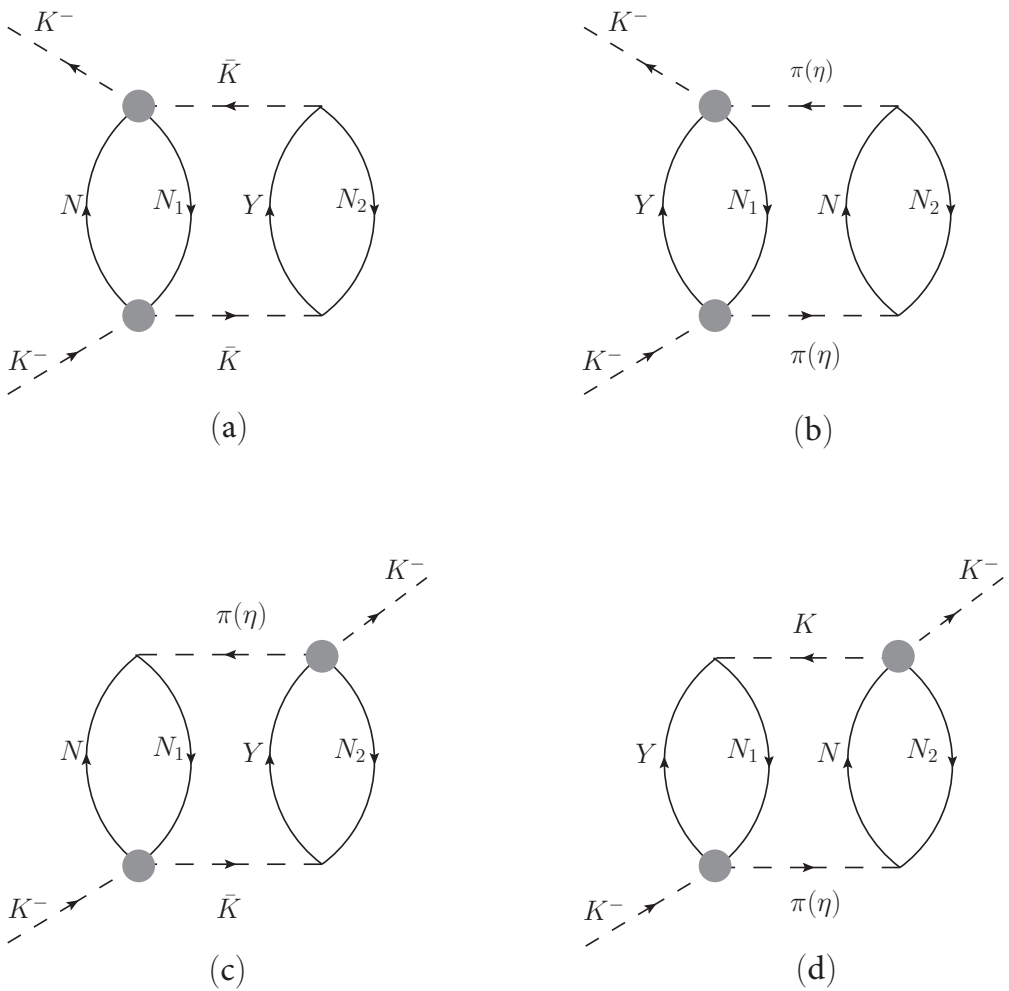

Fig.2: Two-fermion-loop (2FL) Feynman diagrams for non-mesonic K^- absorption on two nucleons N_1, N_2 in nuclear matter. The shaded circles denote the K^-N t-matrices derived from a chiral model.

K^-NN absorption in nuclear matter

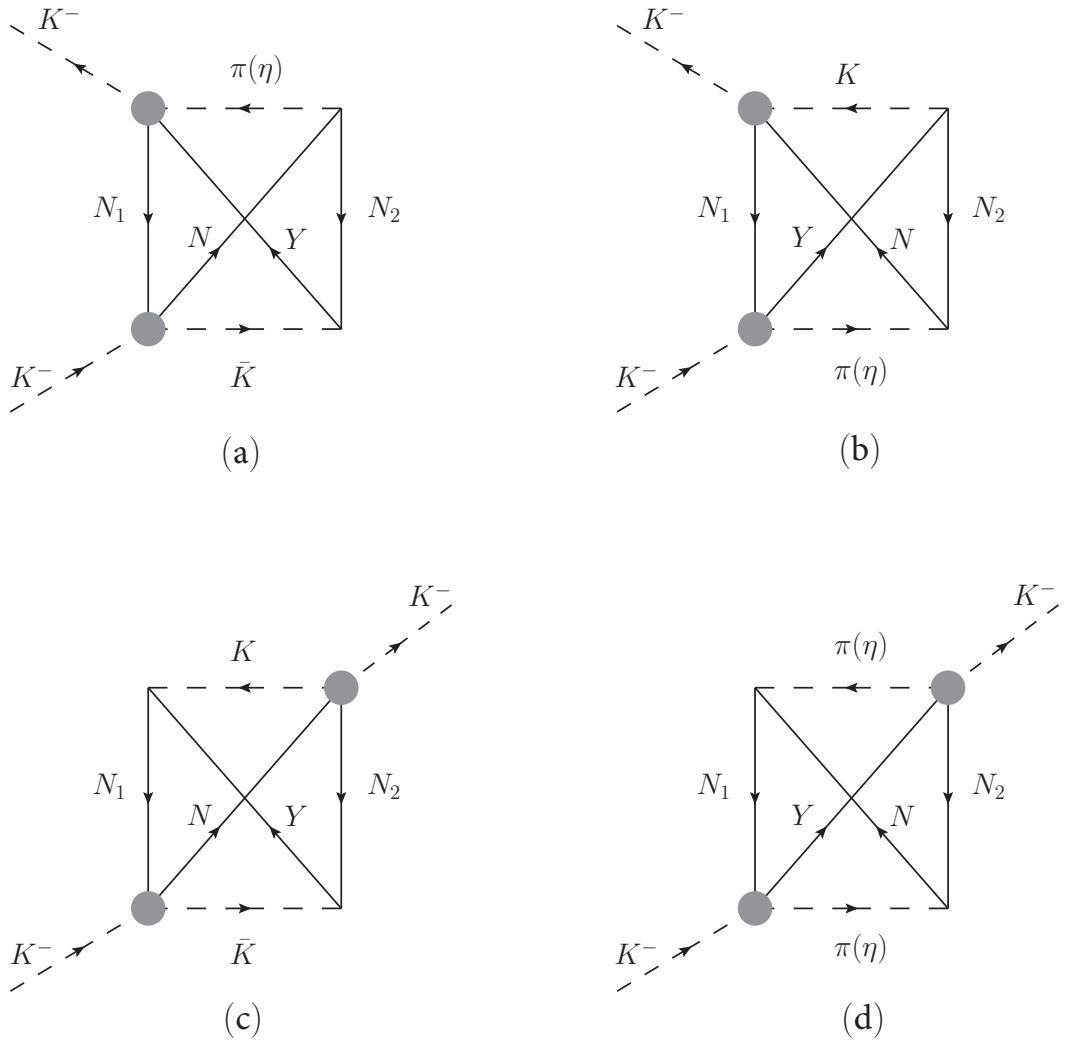

Fig.3: One-fermion-loop (1FL) Feynman diagrams for non-mesonic K^- absorption on two nucleons N_1, N_2 in nuclear matter. The shaded circles denote the K^-N t-matrices derived from a chiral model.

K^-NN absorption in nuclear matter

$V_{K^-N} = \sum_{channels} V_{K^-N\to\pi Y}$ (Fig.1)

$V_{K^-NN} = \sum_{\text{channels}} V^{\text{2FL}}_{K^-NN} + V^{\text{1FL}}_{K^-NN}$ (Fig.2 and 3)

$\to$ contributions from 37 2FL and 28+33 1FL diagrams

Table 1: All considered channels for mesonic and non-mesonic K^- absorption in matter.

K^-N	$\to \pi Y$	$K^-N_1N_2$	$\to YN$
K^-p	$\to \pi^0\Lambda$	K^-pp	$\to \Lambda p$
	$\to \pi^0\Sigma^0$		$\to \Sigma^0 p$
	$\to \pi^+\Sigma^-$		$\to \Sigma^+ n$
	$\to \pi^-\Sigma^+$	$K^-pn(np)$	$\to \Lambda n$
K^-n	$\to \pi^-\Lambda$		$\to \Sigma^0 n$
	$\to \pi^-\Sigma^0$		$\to \Sigma^- p$
	$\to \pi^0\Sigma^-$	K^-nn	$\to \Sigma^- n$

AMADEUS: Ratio for 2N absorption

Recently measured ratio *R. Del Grande et al., EPJ C79 (2019) 190*

$$R = \frac{\mathrm{BR}(K^- pp \to \Lambda p)}{\mathrm{BR}(K^- pp \to \Sigma^0 p)} = 0.7 \pm 0.2(\mathrm{stat.})^{+0.2}_{-0.3}(\mathrm{syst.})$$

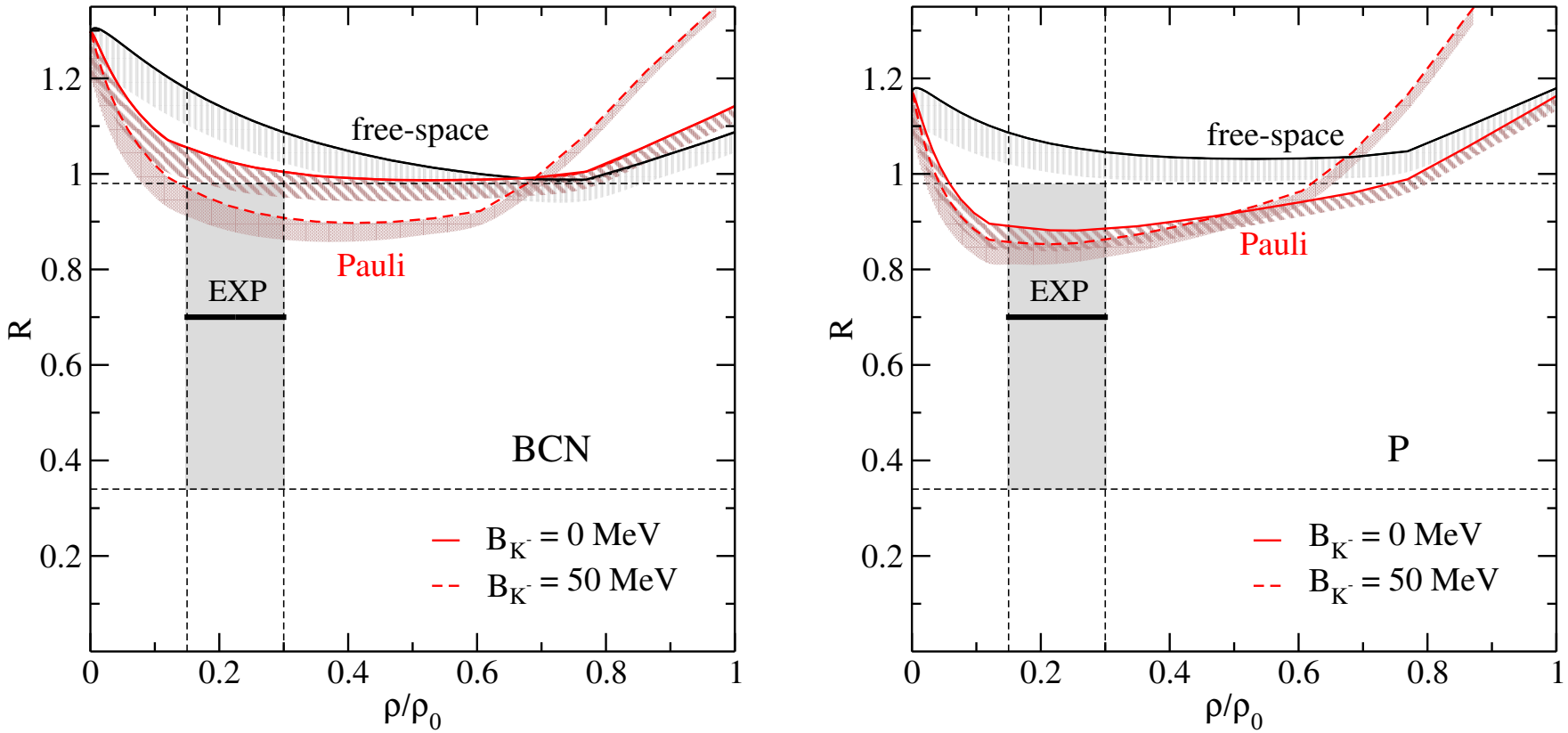

Fig.4: The ratio R as a function of relative density, calculated using the free-space and Pauli blocked amplitudes for $B_{K^-} = 0$ MeV and $B_{K^-} = 50$ MeV. Color bands denote the uncertainty due to different cut-off values $\Lambda_c = 800 - 1200$ MeV.

Application to kaonic atoms

J. Óbertová, E. Friedman, J. Mareš, PRC 106 (2022) 065201

- K^-NN model applied in calculations of energy shifts and widths in kaonic atoms
- BCN amplitudes used $\rightarrow$ in-medium modifications included (Pauli or WRW *T. Wass, M. Rho, W. Weise, NPA 617 (1997) 449*)
- microscopic $K^-N + K^-NN$ potentials calculated for 23 targets and confronted with kaonic atom data
- $K^-N + K^-NN$ potentials then supplemented by a phenomenological term describing 3 and 4 nucleon processes $\sim -4\pi B(\frac{\rho}{\rho_0})^\alpha \rho$
- values of α and complex amplitude B fitted to data

Confrontation with kaonic atom data

Table 2: Values of $\chi^2(65)$ resulting from comparison of predictions with kaonic atom data using K^-N, $K^-N + K^-NN$, and $K^-N + K^-NN$+phen. multiN potentials. Values of complex amplitude B and parameter α for potentials based on Pauli blocked and WRW modified BCN amplitudes.

	K^-N	$K^-N + K^-NN$	+ phen.	ReB (fm)	ImB (fm)	α
Pauli	825	565	105	-1.97(13)	-0.93(11)	1.4
WRW	2378	1123	116	-0.90(9)	0.72(10)	0.6

- best fit K^-N + phen. multiN potential based on BCN amplitudes ReB = -1.3 fm, ImB = 1.9 fm, $\alpha = 1$, $\chi^2(65) = 112.3$

Model improvement - hadron self-energies

- inclusion of Y, N, K^- and π self-energies into the K^-N chiral BCN amplitudes as well as into the K^-NN model.
- considered baryon potentials

$$V_N = -70\frac{\rho}{\rho_0}\ ,$$
$$V_\Lambda = -340\rho + 1087.5\rho^2 \ \rightarrow V_\Lambda(\rho_0) = -26.4\ \mathrm{MeV},$$
$$V_\Sigma = 30\frac{\rho}{\rho_0}\ .$$

- considered pion S- and P-wave self-energy

A. Ramos, E. Oset, NPA 671 (2000) 481

Hadron self-energies: $K^- p$ amplitudes

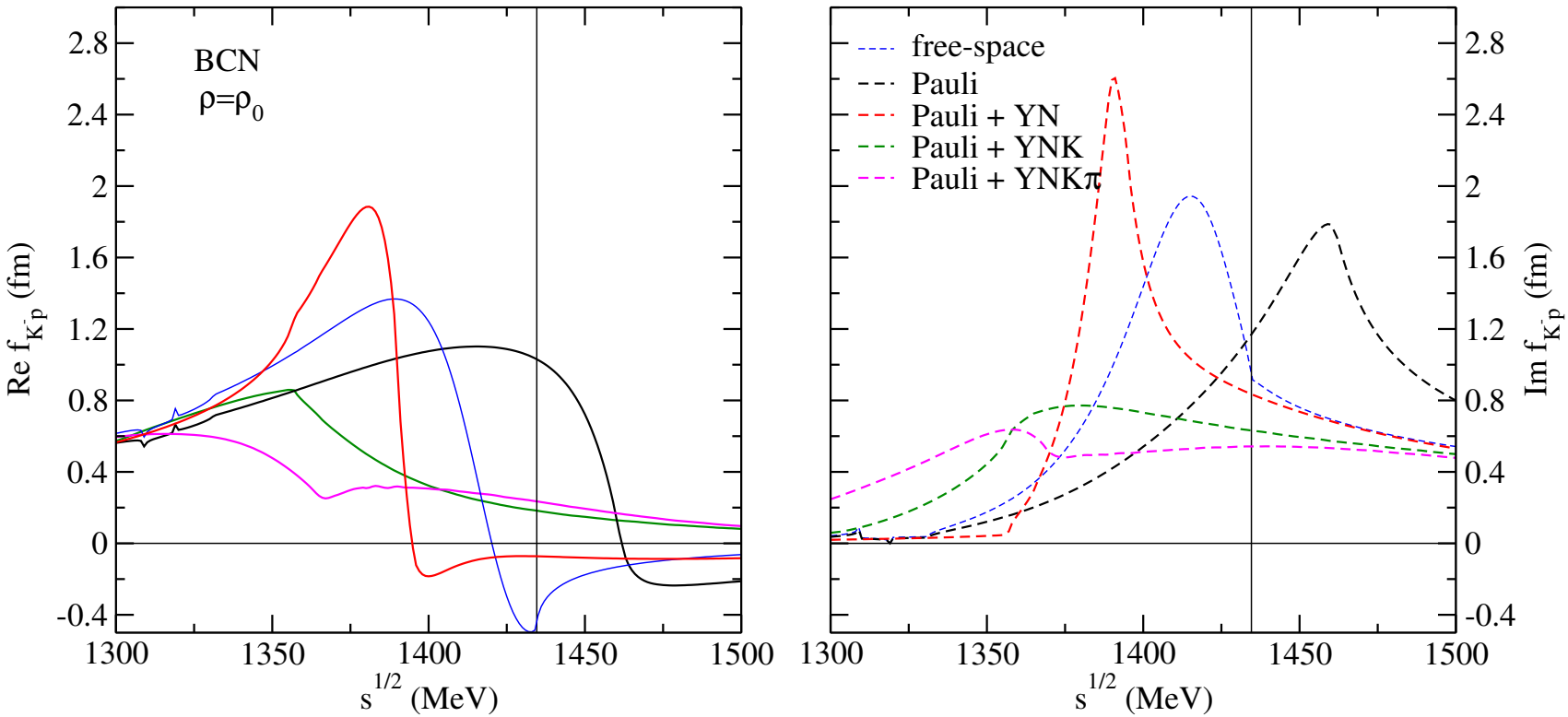

Fig.5: Comparison of $K^- p \to K^- p$ BCN amplitudes with Pauli blocking only (black), Pauli+YN SE (red), Pauli + YNK^- SE (green), and Pauli + $YNK^-\pi$ SE (magenta) at saturation density $\rho_0 = 0.17$ fm^{-3}.

Hadron self-energies: $K^- n$ amplitudes

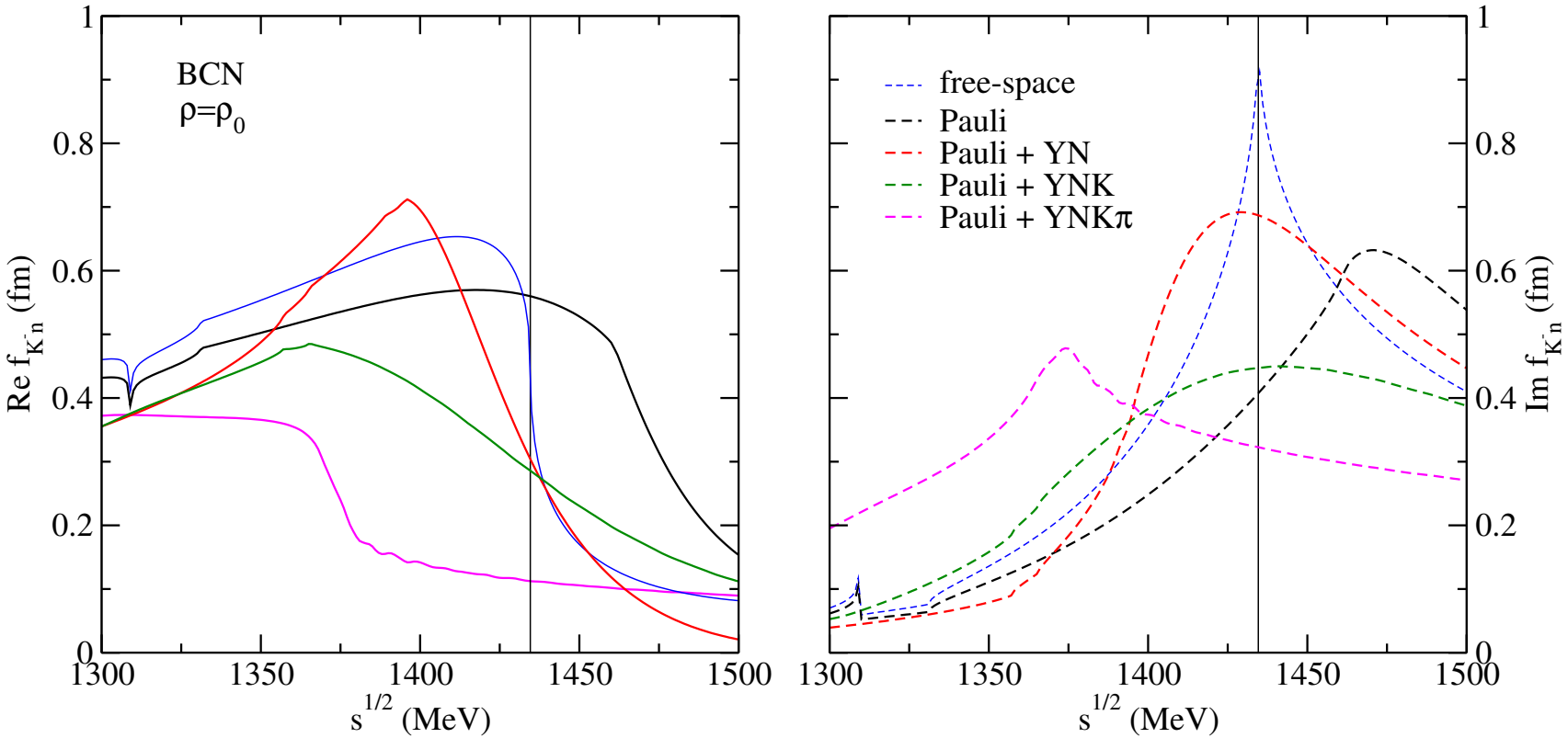

Fig.6: Comparison of $K^- n \to K^- n$ BCN amplitudes with Pauli blocking only (black), Pauli+YN SE (red), Pauli + YNK^- SE (green), and Pauli + $YNK^-\pi$ SE (magenta) at saturation density $\rho_0 = 0.17$ fm^{-3}.

Comparison with AMADEUS measurement

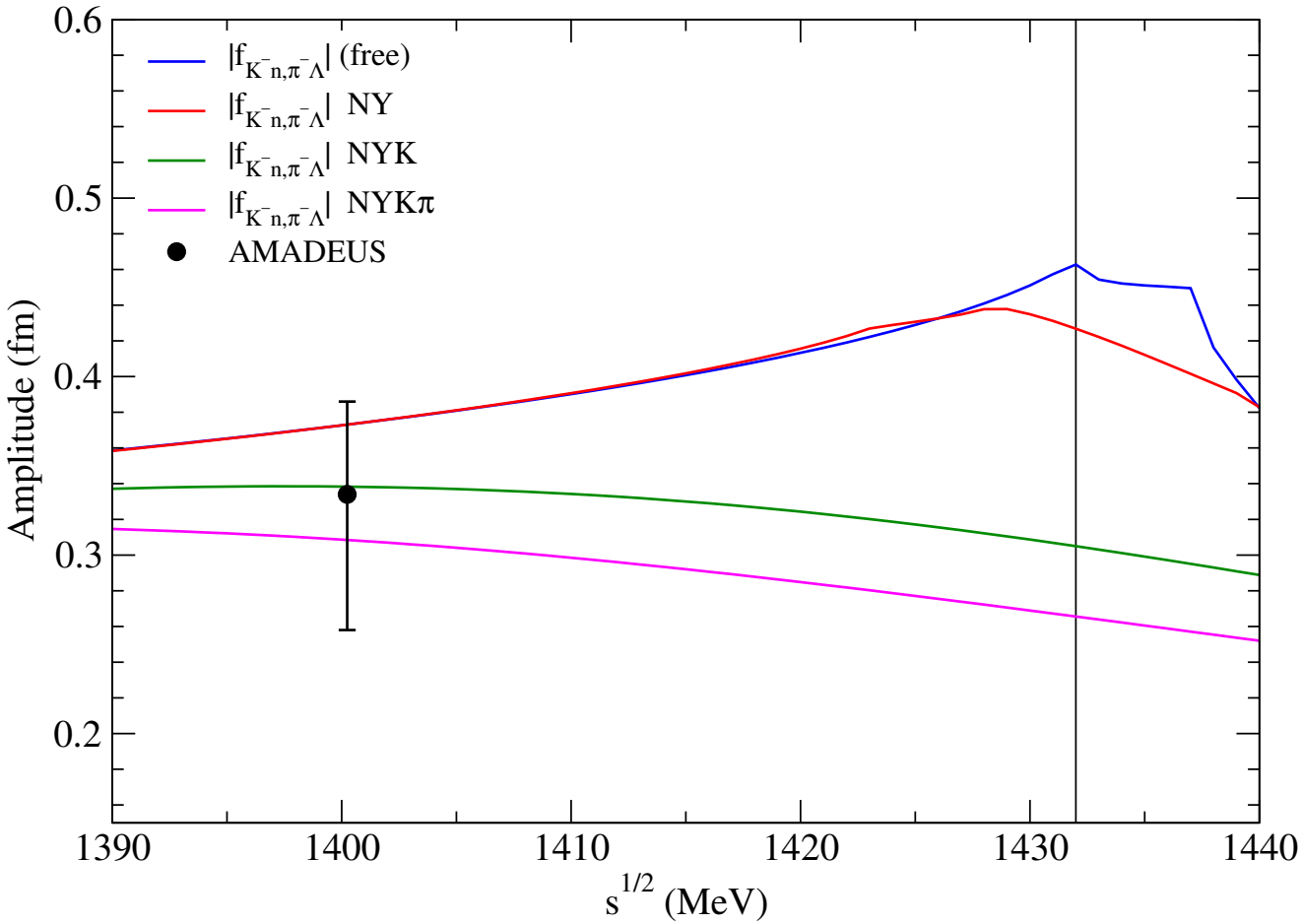

Fig.7: Comparison of $|f_{K^-n\to\pi^-\Lambda}|$ measured by AMADEUS with free-space amplitude from the BCN model (blue) and with in-medium amplitudes: Pauli + *YN* SE (red), Pauli+*YNK* SE (green), and Pauli + $YNK^-\pi$ SE (magenta) from the BCN model (taken at $\rho = 0.3\rho_0$).

Hadron self-energies: K^- potential

- Pauli + YN SE amplitudes $\Rightarrow V_{K^-} = V_{K^-N} + V_{K^-NN}$
- Pauli + $YNK^-(YNK^-\pi)$ SE amplitudes

$$\Downarrow$$

$$V_{K^-} = t\rho + V^{\rm corr}_{K^-NN}$$

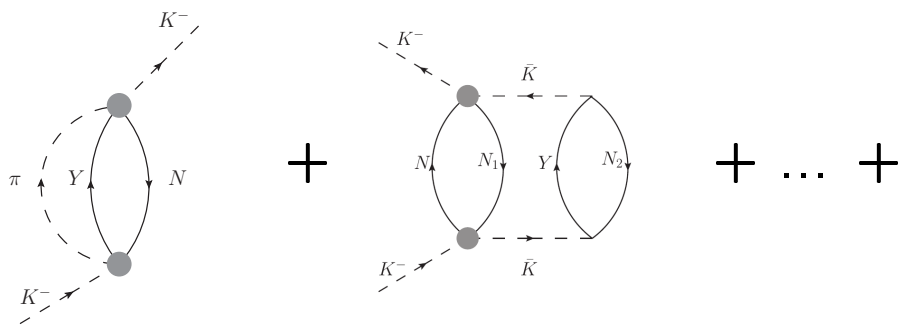

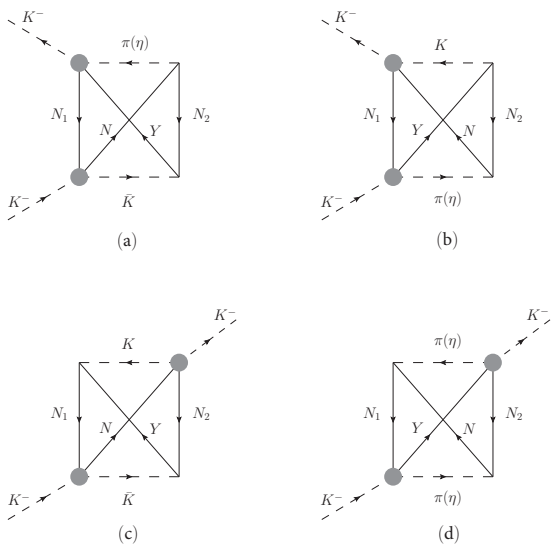

Hadron self-energies: total K^- potential

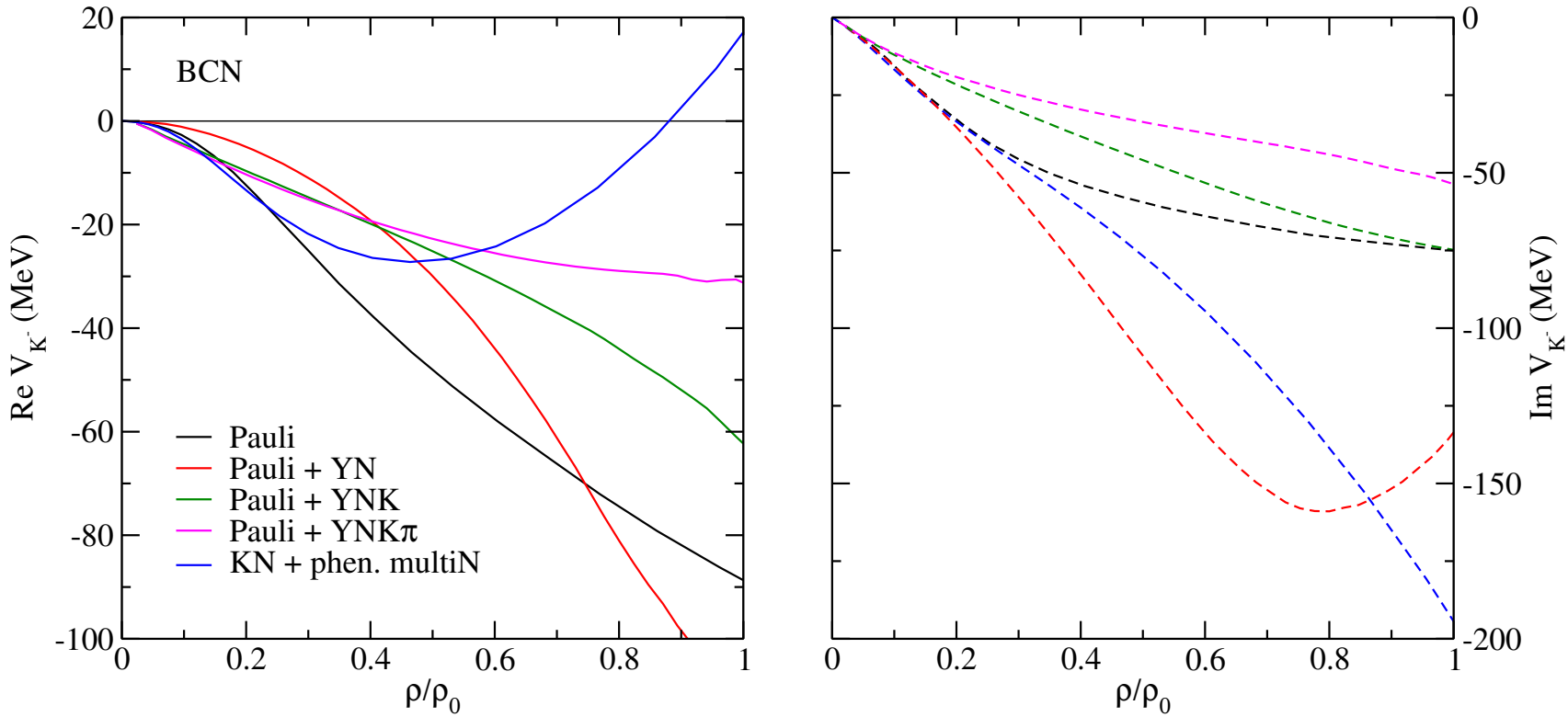

Fig.8: Real (left) and imaginary (right) parts of the total K^- potential as a function of relative density ρ/ρ_0, calculated with Pauli (black), Pauli + *YN* SE (red), Pauli + YNK^- SE (green), and Pauli + $YNK^-\pi$ SE (magenta) BCN amplitudes. For comparison there is the best fit K^-N + phen. multiN potential (blue) based on BCN amplitudes.

Calculations of selected kaonic atoms

Table 3: Values of χ^2 for shifts, widths and yields in selected K^- atoms, calculated with Pauli + YN, Pauli + YNK, Pauli + YNKπ BCN amplitudes and with K^-N+phen. multiN potentials based on BCN WRW amplitudes.

BCN		Pauli + YN	Pauli + YNK	Pauli + YNKpi	phen.
		$K^-N + K^-NN$	$t\rho + V^{corr}_{K^-NN}$	$t\rho + V^{corr}_{K^-NN}$	K^-N + phen. multiN
^{12}C	$\Delta(\epsilon)$	0.81	0.02	0.36	1.76
	Γ	17.48	3.15	0.00	0.70
	Γ^*	3.98	3.08	3.46	2.74
^{31}P	$\Delta(\epsilon)$	1.84	0.15	0.01	0.03
	Γ	12.85	2.49	0.18	0.24
	Γ^*	0.08	0.03	0.02	0.30
^{32}S	$\Delta(\epsilon)$	25.48	7.80	2.28	1.24
	Γ	74.33	23.85	7.05	9.24
	Γ^*	0.43	0.06	0.08	0.47
^{35}Cl	$\Delta(\epsilon)$	0.86	0.03	0.02	2.10
	Γ	12.35	1.28	0.14	0.00
	Γ^*	0.06	0.05	0.07	0.15
^{63}Cu	$\Delta(\epsilon)$	0.06	2.04	5.12	3.19
	Γ	7.73	2.71	0.98	2.25
	Γ^*	2.79	1.86	1.81	1.52
^{118}Sn	$\Delta(\epsilon)$	5.59	1.44	0.74	2.15
	Γ	1.33	0.41	0.11	0.29
	Γ^*	2.97	3.55	3.81	4.09
^{208}Pb	$\Delta(\epsilon)$	3.36	0.04	0.87	0.34
	Γ	0.49	0.39	0.33	0.39
	Γ^*	0.46	0.54	0.57	0.52
$\chi^2(21)$	total	175.34	54.98	28.00	33.71
χ^2/d.p.	total	8.35	2.62	1.33	1.61
$\chi^2(18)$	S^{32} out	75.10	23.27	18.60	22.76
χ^2/d.p.	S^{32} out	4.17	1.29	1.03	1.26

Calculated branching ratios in $^{12}C+K^-$ atom

Table 4: Primary-interaction branching ratios (in %) for mesonic ($K^-N \to Y\pi$, $Y = \Lambda, \Sigma$) and non-mesonic absorption ($K^-NN \to YN$) of K^- in $^{12}C+K^-$ atom (I=2), calculated with $K^-N + K^-NN$ potentials based on WRW, Pauli blocked, and Pauli+YN BCN amplitudes.The experimental data corrected for primary interaction are shown for comparison.

$^{12}C + K^-$ (I=2)	BCN			Exp.
mesonic ratio	WRW	Pauli	Pauli + YN	^{12}C [1]
$\Sigma^+\pi^-$	26.9	22.4	17.0	29.4 ± 1.0
$\Sigma^-\pi^0$	8.3	7.7	8.7	2.6 ± 0.6
$\Sigma^-\pi^+$	15.5	17.5	22.3	13.1 ± 0.4
$\Sigma^0\pi^-$	8.4	7.9	8.8	2.6 ± 0.6
$\Sigma^0\pi^0$	17.2	16.4	16.4	20.0 ± 0.7
$\Lambda\pi^0$	5.2	5.0	5.3	3.4 ± 0.2
$\Lambda\pi^-$	10.4	9.9	11.5	6.8 ± 0.3
total 1N ratio	91.9	87.0	90.0	77.9 ± 1.6
non-mesonic ratio	WRW	Pauli	Pauli + YN	76% CF_3Br + 24% C_3H_8 [2]
$\Lambda p + \Lambda n + \Sigma^0 p + \Sigma^0 n$	4.2	6.7	5.0	14.1 ± 2.5 [a]
$\Sigma^- p + \Sigma^- n$	1.7	3.1	3.4	7.3 ± 1.3 [a]
$\Sigma^+ n$	2.2	3.5	1.7	4.3 ± 1.2 [a]
$\Sigma^0 p + \Sigma^0 n$	1.9	3.1	2.4	-
total 2N ratio	8.1	13.0	10.0	$16 \pm 3(\text{stat.})^{+4}_{-5}(\text{syst.})$ [3]

[a] multinucleon capture rate

[1] *C. Vander Velde-Wilquet et al., NC 39 A (1977) 538*

[2] *H. Davis et al., NC 53 A (1968) 313*

[3] *R. Del Grande et al., EPJ C79 (2019) 190*

Calculated branching ratios in $^{12}C+K^-$ atom

Table 5: Primary-interaction branching ratios (in %) for mesonic ($K^-N \to Y\pi$, $Y = \Lambda, \Sigma$) and non-mesonic absorption of K^- in $^{12}C+K^-$ atom (I=2), calculated with potentials based on Pauli+*YNK* and Pauli+*YNK*π BCN amplitudes.The experimental data corrected for primary interaction are shown for comparison.

$^{12}C + K^-$ (I=2)	BCN		Exp.
mesonic ratio	Pauli+YNK	Pauli+YNKπ	^{12}C [1]
$\Sigma^+\pi^-$	15.8	14.4	29.4 $\pm$ 1.0
$\Sigma^-\pi^0$	8.3	8.1	2.6 $\pm$ 0.6
$\Sigma^-\pi^+$	14.1	12.8	13.1 $\pm$ 0.4
$\Sigma^0\pi^-$	8.4	8.2	2.6 $\pm$ 0.6
$\Sigma^0\pi^0$	11.4	10.0	20.0 $\pm$ 0.7
$\Lambda\pi^0$	5.3	5.3	3.4 $\pm$ 0.2
$\Lambda\pi^-$	11.2	11.1	6.8 $\pm$ 0.3
total 1N ratio	74.3	70.0	77.9 $\pm$ 1.6
total multiN ratio	25.7	30.0	25.7 $\pm$ 3.1 [2] 21 $\pm$ 3(stat.)$^{+5}_{-6}$(syst.) [3]

[1] *C. Vander Velde-Wilquet et al., NC 39 A (1977) 538*
[2] *H. Davis et al., NC 53 A (1968) 313*
[3] *R. Del Grande et al., EPJ C79 (2019) 190*

Summary

- K^-N interaction described by chiral meson-baryon coupled channel interaction models
- Chiral K^-N interaction models are unable to describe kaonic atom data
- Interactions of K^- with two and more nucleons important for realistic description of the K^--nucleus interaction
  - only P, KM, and BCN models compatible with available data
- We have developed a microscopic model for K^-NN absorption in nuclear matter using amplitudes derived from the P and BCN chiral meson-baryon interaction models

  J. Hrtánková, À. Ramos, PRC 101 (2020) 035204
  - Pauli blocked amplitudes included $\rightarrow$ medium effects non-negligible

Summary

- Microscopic $K^-N + K^-NN$ potentials based on Pauli blocked BCN ampplitudes confronted with kaonic atom data *J. Óbertová, E. Friedman, J. Mareš, PRC 106 (2022) 065201*
  - the description of kaonic atoms improves considerably when microscopic K^-NN potentials are included (χ^2 drops down twice)
- Further improvement of the K^-NN model and K^-N BCN amplitude model $\rightarrow$ inclusion of hadron (Y, N, K^-, π) self-energies
- Considering K^- and π SE $\rightarrow$ $\mathrm{Im}\, V_{K^-}(\rho_0) \sim -75$ and -50 MeV
- Calculations of selected kaonic atoms $\rightarrow$ **full model Pauli+$YNK\pi$ SE describes the data as good as the best fit K^-N+phen. multiN potential based on BCN amplitudes!**